



UNIVERSITÀ
DEGLI STUDI
FIRENZE

FLORE

Repository istituzionale dell'Università degli Studi di Firenze

Interactions between mid-ocean ridge and subduction magmatism in Albanian ophiolites

Questa è la Versione finale referata (Post print/Accepted manuscript) della seguente pubblicazione:

Original Citation:

Interactions between mid-ocean ridge and subduction magmatism in Albanian ophiolites / V. BORTOLOTTI; M. MARRONI; L. PANDOLFI; G. PRINCIPI; E. SACCANI. - In: THE JOURNAL OF GEOLOGY. - ISSN 0022-1376. - STAMPA. - 110:(2002), pp. 561-576.

Availability:

The webpage <https://hdl.handle.net/2158/311384> of the repository was last updated on

Terms of use:

Open Access

La pubblicazione è resa disponibile sotto le norme e i termini della licenza di deposito, secondo quanto stabilito dalla Policy per l'accesso aperto dell'Università degli Studi di Firenze (<https://www.sba.unifi.it/upload/policy-oa-2016-1.pdf>)

Publisher copyright claim:

La data sopra indicata si riferisce all'ultimo aggiornamento della scheda del Repository FloRe - The above-mentioned date refers to the last update of the record in the Institutional Repository FloRe

(Article begins on next page)

Interaction between Mid-Ocean Ridge and Subduction Magmatism in Albanian Ophiolites

V. Bortolotti, M. Marroni,¹ L. Pandolfi,² G. Principi, and E. Saccani³

Dipartimento di Scienze della Terra, Università di Firenze, via La Pira 4, 50121 Firenze, Italy

ABSTRACT

Albanian ophiolites are represented by two different coeval belts, each displaying well-exposed, complete ophiolitic sequences that originated in the same oceanic basin and each showing distinct geochemical characteristics. The eastern belt is characterized by suprasubduction zone (SSZ) ophiolitic sequences, including island arc tholeiitic and boninitic volcanic series. The western belt, although composed mainly of mid-ocean ridge-type (MOR-type) ophiolites with high-Ti geochemical affinity, also exhibits alternating sequences showing distinct geochemical affinities referable to MOR- and SSZ-type volcanics. These volcanics can be geochemically subdivided into four groups: (1) group 1 basalts show high field strength element (HFSE) and rare earth element (REE) concentrations similar to those of ocean-floor basalts; (2) group 2 basalts, basaltic andesites, dacites, and rhyolites, characterized by HFSE and light REE depletion similar to those in many low-Ti volcanics from SSZ settings; (3) group 3 basalts exhibit geochemical features intermediate between groups 1 and 2 but also bear SSZ features, being characterized by HFSE depletion with respect to the N-MORBs; (4) group 4 boninitic dikes display very low-Ti contents and typically depleted, U-shaped REE patterns. These different magmatic groups are interpreted as having originated from fractional crystallization from different primary basalts that were generated, in turn, from partial melting of mantle sources progressively depleted by previous melt extractions. Consequently, group 1 basalts may derive from partial melting of a fertile MORB source, while group 3 basalts may derive from 10% partial melting of a mantle that previously experienced MORB extraction. Finally, the group 2 basalts and group 4 boninites may be derived from about 10% partial melting of a mantle peridotite previously depleted by primary melt extraction of group 1 and group 3 primary melts. To explain the coexistence of these geochemically different magma groups, we present a model based on the complexity of the magmatic processes that may take place during the initiation of subduction in proximity to an active MOR. This model implies that the initiation of subduction processes close to such a ridge leads to contemporaneous eruptions in a fore-arc setting of MORBs (group 1) generated from the extinguishing MOR and the initiation of group 3 basalts generated in the SSZ mantle wedge from a moderately depleted mantle source. The development of the subduction in a young, hot lithosphere caused the generation of island arc tholeiitic basalts (group 2) and boninites (group 4) from strongly depleted mantle peridotites in the early stages of subduction, soon after the generation of group 1 and group 3 basaltic rocks.

Introduction

Geochemical and geological studies on ophiolites reveal the occurrence of magmatic suites generated in various geodynamic settings. Ophiolites were initially regarded as a typical oceanic crust formed at mid-ocean ridge (MOR) spreading centers. However, additional data on worldwide ophiolites as well as

studies of modern oceanic basins indicate that intraoceanic subduction is an important process in the formation of ophiolitic complexes known as supra-subduction zone (SSZ) ophiolites (Pearce et al. 1984). In both MOR and SSZ settings, further subdivisions can be found; for instance, in SSZ ophiolites island arc, back-arc, or fore-arc subtypes can be recognized. In many cases the original geodynamic settings are very difficult to distinguish; thus a complete set of petrological, geochemical, and geological data need to be taken into account for a more effective discrimination. Additional problems occur in ophiolitic sequences where rocks showing distinctive geochemical features coexist either spatially or tem-

Manuscript received July 31, 2001; accepted October 2, 2001.

¹ Present address: Dipartimento di Scienze della Terra, Università di Pisa, via S. Maria 53, 56126 Pisa, Italy.

² Istituto di Geoscienze e Georisorse, via S. Maria 53, 56126 Pisa, Italy.

³ Author for correspondence. Present address: Dipartimento di Scienze della Terra, Università di Ferrara, Corso Ercole I d'Este 32, 44100 Ferrara, Italy; e-mail: sac@unife.it.

porally or else are interlayered in the same ophiolitic sequence as, for instance, the Zambesi ophiolites (Geary et al. 1989; Yumul 1996) and the southern Chile Ridge–Taitao ophiolites (Klein and Karsten 1995).

Albanian ophiolites occur in a large nappe consisting of two different belts (Beccaluva et al. 1994), the eastern and western ophiolitic belts, each displaying well-exposed, complete ophiolitic sequences. These sequences probably originated in the same oceanic basin, as indicated by the occurrence of a common sedimentary cover as well as a common metamorphic sole (Bortolotti et al. 1996). Moreover, they are separated by pre-Barremian thrusts; this fact also suggests a Jurassic contiguous position of these belts. A SSZ geochemical signature characterizes the eastern belt, whereas in the western belt, MOR- and SSZ-type volcanics alternate (Bortolotti et al. 1996; Bébien et al. 2000).

Bortolotti et al. (1996) interpreted the contemporaneous presence of different magma types in the western ophiolitic belt as the result of magmatic processes developed in a young MOR-type crust in a proto-fore-arc region. By contrast, Bébien et al. (2000) concluded that western- and eastern-type ophiolites cannot be related to a definite tectonic setting (either MOR or SSZ). In their model, Bébien et al. (2000) suggest that both ophiolitic types are related to an early stage of subduction. However, this conclusion is somewhat in contrast with the general consensus that in the Albanian ophiolites (Beccaluva et al. 1994; Shallo 1994; Cortesogno et al. 1998), as in all the Dinaride-Hellenide ophiolites (Jones et al. 1991; Robertson and Shallo 2000), the high-Ti and low-Ti ophiolitic belts reflect two distinct original geodynamic settings referred to as MOR and SSZ, respectively.

In this article, we provide new geological and petrological evidence of the coexistence in the same ophiolitic sequences of interlayered, different magmatic suites. In addition, we propose a new geodynamic model for the Albanian ophiolites concerning the development of such a composite oceanic crust as a consequence of a complex interaction between different tectonomagmatic settings.

Geological Setting

Albanian ophiolites occur as a 250-km-long, NNW-SSE-trending nappe (Mirdita Nappe) emplaced onto the continental sequences of the Adria plate and represent the suture zone formed during the progressive closure of the Jurassic Tethyan oceanic basin between the Adria and Eurasia plates (Robert-

son and Dixon 1984) (fig. 1A). As in many other eastern Mediterranean ophiolitic belts, an assemblage of oceanic- and continental-derived thrust sheets (Rubik Mélange) occurs at the base of the ophiolitic nappe (Bortolotti et al. 1996). The ophiolites are in turn unconformably overlain by Late Jurassic–Early Cretaceous sediments (fig. 2), which are referred to as the “Simoni Mélange” and “Firza Flysch” (Bortolotti et al. 1996).

On the basis of geological, petrological, and metallogenic data (Beccaluva et al. 1994; Shallo 1994), the Albanian ophiolites are subdivided in two sub-parallel belts: the eastern and the western ophiolitic belts, which are delimited by a post-Valanginian high-angle thrust (figs. 1B, 2). The eastern ophiolitic belt shows a well-developed, 6–8-km-thick sequence including, from bottom to top, harzburgitic mantle tectonites, ultramafic cumulates (chromite-bearing dunites, chromitites, dunites, olivine-websterites, and websterites), mafic cumulates (olivine-gabbro-norites, gabbro-norites, and isotropic gabbros), quartz-diorites and plagiogranites, a sheeted dike complex, and a volcanic sequence (including massive and pillow-lava basalts, basaltic andesites, andesites, dacites, and rhyolites) with an apparent thickness of ca. 1200 m.

These ophiolites have a very low- and low-Ti geochemical character with island arc tholeiitic (IAT) and boninitic affinities that suggest their origin in an SSZ setting (Beccaluva et al. 1994). They are similar to most Mesozoic Tethyan ophiolites, for example, Troodos (Kostopoulos and Murton 1992), Vourinos (Rassios et al. 1983), Pindos (Jones et al. 1991), and Oman (Rochette et al. 1991). Nonetheless, the sporadic occurrence of MOR-like rocks has been described (Beccaluva et al. 1994; Bébien et al. 1998) in the lower cumulates; these consist of few layers of troctolites (up to 50 cm thick) included in the upper part of the ultramafic cumulates.

In contrast, the western ophiolitic belt is characterized by a 3–4-km-thick sequence that includes, from bottom to top, lherzolitic mantle tectonites, a layered mafic-ultramafic cumulate sequence (plagioclase-dunites, dunites, troctolites, plagioclase-whelrlites, wherlites, gabbros and scarce Fe-gabbros, diorites, and plagiogranites), and a volcanic sequence (estimated maximum thickness ca. 300–400 m) mainly composed of high-Ti pillow-lava basalts of MORB affinity (Beccaluva et al. 1994). A sheeted dike complex is recognized in only a few areas. The overall petrographical and geochemical characteristics, analogous to those observed in mid-ocean ridges, indicate that this ophiolitic belt originated in a similar setting (Shallo 1994). Geological evidence suggesting a back-arc origin for the western-belt

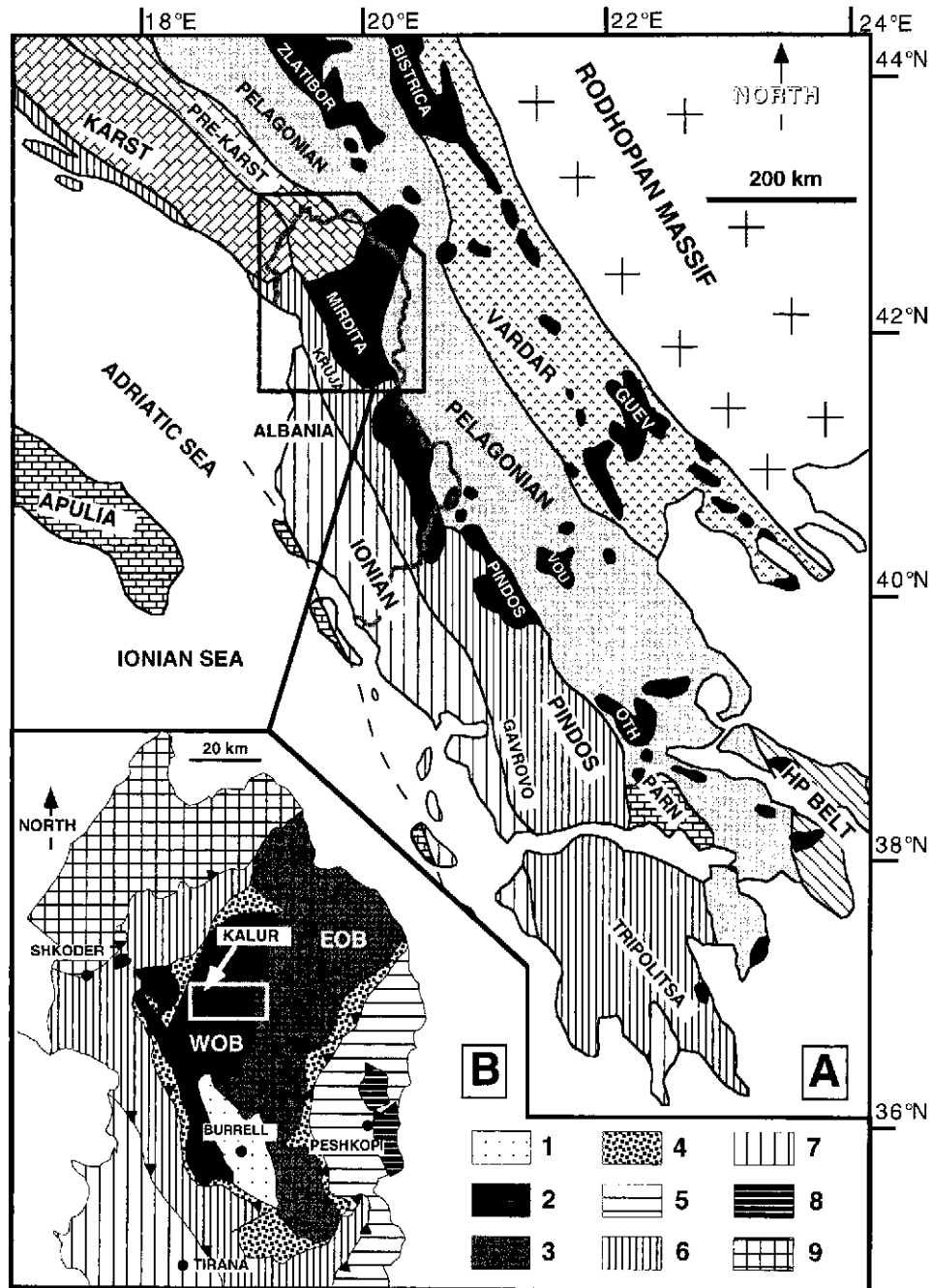


Figure 1. A, Tectonic scheme and location of the major ophiolitic massifs (solid black) for the Dinaric-Hellenic Belt, modified after Aubouin et al. (1970). Abbreviations: *Guev* = Guevgueli; *Vou* = Vourinos; *Oth* = Othris; *Parn* = Parnassus Zone. B, Schematic geological setting of the northern Albania and central Mirdita areas. 1 = Late Tertiary molasse deposits; 2 = western-belt ophiolite sequence (WOB); 3 = eastern-belt ophiolite sequence (EOB); 4 = Rubik Mélange; 5 = Pelagonian Units; 6 = Krasta-Çucali Unit; 7 = Kruja Unit; 8 = units of the Peshkopi Window; 9 = Albanian Alps. Box indicates the investigated area.

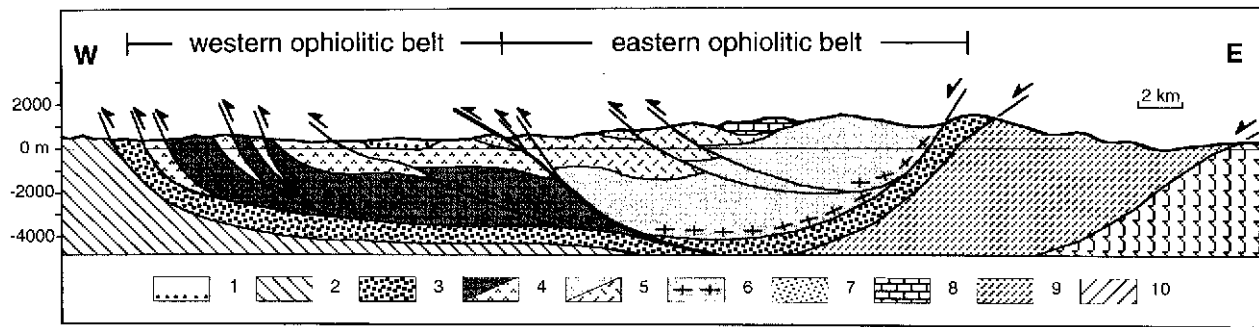


Figure 2. Schematic cross-section of the Albanian ophiolites in the Mirdita area. 1 = Late Tertiary molasse deposits; 2 = Adria continental units (Krasta-Çucali and Kruja Units); 3 = Rubik Mélange; 4 = western-belt ophiolites (*upper half*, mantle section; *lower half*, crustal section); 5 = eastern-belt ophiolites (*upper half*, mantle section; *lower half*, crustal section); 6 = metamorphic sole; 7 = Simoni Mélange and Firza Flysch; 8 = Barremian carbonate deposits; 9 = Pelagonian Units; 10 = units of the Peskhopi Window.

ophiolites has never been presented in the literature (Beccaluva et al. 1994; Shallo 1994; Bortolotti et al. 1996; Cortesogno et al. 1998; Robertson and Shallo 2000). The reduced thickness of this ophiolitic sequence and the rare occurrence of sheeted dike complexes suggest the western belt originated in a slow-spreading ridge (Cortesogno et al. 1998).

In addition to the MOR-type basalts, the volcanic sequence of the western belt also includes (i) volcanic rocks with geochemical features intermediate between MOR and IAT, (ii) typical IAT volcanic rocks, and (iii) very low-Ti basaltic dikes (Bortolotti et al. 1996; Bébien et al. 2000). Consequently, the western belt represents an ophiolitic sequence in which volcanics with different geochemical characteristics coexist.

Both western and eastern ophiolitic sequences are topped by similar sedimentary sequences (i.e., Rubik Cherts, Simoni Mélange, and Firza Flysch) and are underlain by a geochemically homogeneous metamorphic sole (Carosi et al. 1996; fig. 2). Ages of both western- and eastern-belt metamorphic soles (Vérgely et al. 1998) and sedimentary covers (Marcucci and Prella 1996) are barely distinguishable, suggesting that these two ophiolitic belts originated in the same oceanic basin and were simultaneously involved during the same orogenic phases.

Sampling and Methods

In order to investigate the geochemical variability of volcanics and dikes in the western ophiolitic belt and the geochemical variations between the western and eastern belts, we collected about 100 samples of volcanic and subvolcanic rocks from the central Mirdita area and across the critical contact between

the western and eastern ophiolitic belts (fig. 1B). In particular, we studied in detail a very thick and slightly tectonized volcanic section in the Kalur area (figs. 1B, 2). In this area, an 800-m-thick continuous sequence of basalts (fig. 3) crops out along the Gazuj River. This section consists of up to 50–60-m-thick pillow-lava flows; occasionally a few meters of pillow breccia can be recognized at their top. A 10-m-thick gabbro-bearing sedimentary breccia is interlayered within the volcanic sequence (fig. 3). This volcanic sequence is overlain by the Late Bajocian/Middle Bathonian–Early Callovian Kalur Cherts (Marcucci and Prella 1996). We carried out detailed sampling of this section to investigate its geochemical variations (fig. 3).

We performed bulk-rock major and trace elements analyses with x-ray fluorescence and inductively coupled plasma-mass spectrometry (ICP-MS). Chemical data are given in tables 1 and 2. (Tables 1–3 are available from *The Journal of Geology's* Data Depository free of charge upon request). We carried out chemical analyses on clinopyroxenes with an electron microprobe. Data are presented in table 3.

Petrography and Geochemistry

All samples have been subjected to various degrees of ocean-floor hydrothermal alteration under low- to intermediate-greenschist facies conditions. This alteration has often resulted in extensive reorganization of the primary igneous phases, including replacement of plagioclase by albite or clay minerals and transformation of clinopyroxene into Fe-actinolite or chlorite. Nonetheless, primary igneous textures are usually preserved. Most of the high-Ti ba-

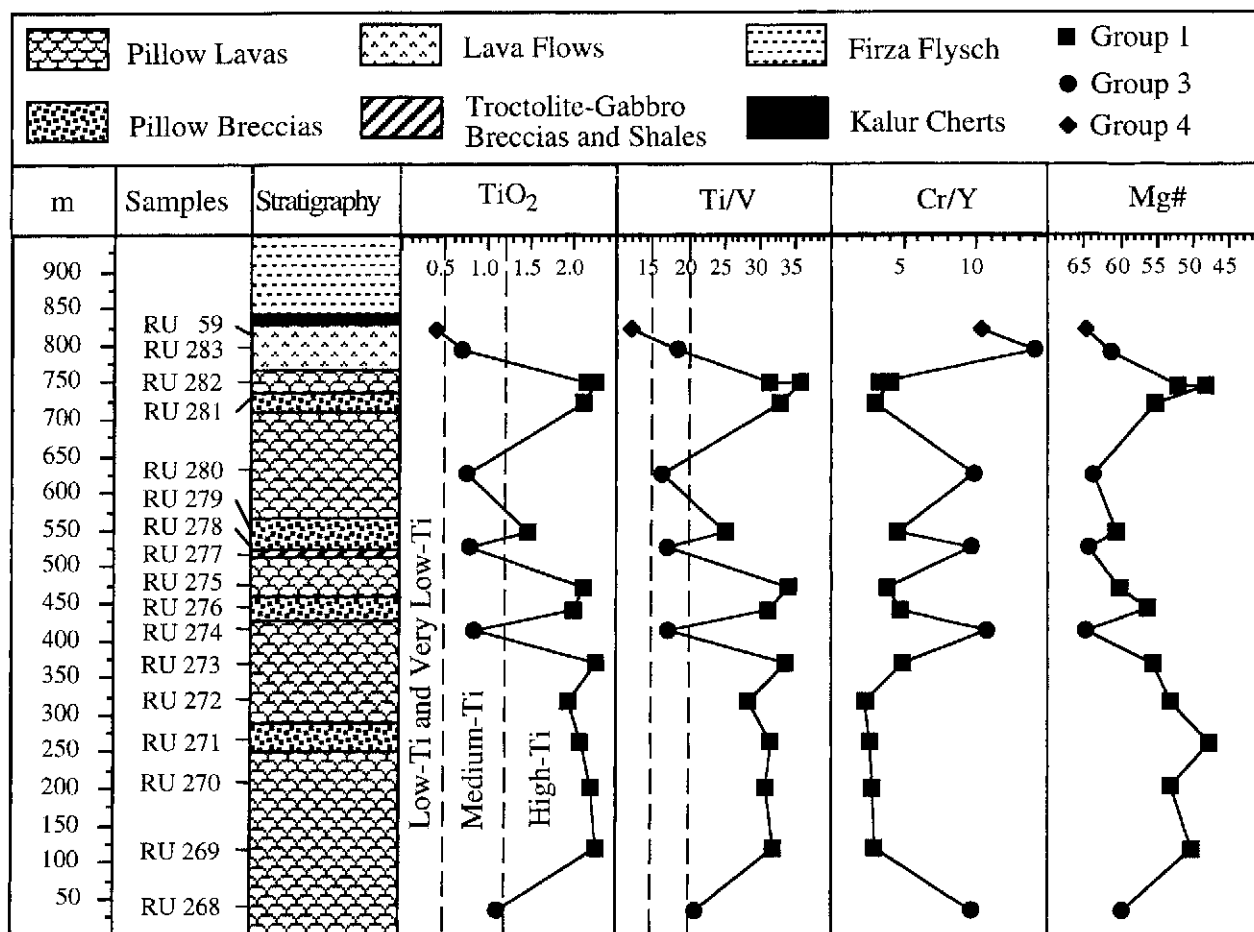


Figure 3. Simplified stratigraphical sequence of the Kalur volcanic section (western ophiolitic belt) and location of studied samples. The variations of representative geochemical parameters along the sequence are also reported. Tie-lines do not indicate continuous geochemical variations. For the geochemical groups, see figure 4.

salts show rather uniform textures, ranging from fine-grained aphyric, with quench laths of plagioclase, to intersertal and intergranular; only a few samples are plagioclase-clinopyroxene porphyritic.

Low-Ti basalts and basaltic andesites display a wide range of textures varying from aphyric to porphyritic ($PI = 5-40$) with phenocrysts of clinopyroxene and plagioclase set in an intergranular to intersertal groundmass. Subophitic textures are also observed in some samples. Andesites and dacites are more porphyritic than basalts. Phenocrysts include clinopyroxene (20%) and plagioclase (30%), with the addition of quartz in dacites. Sporadically, amygdaloidal and glomeroporphyritic textures are found.

The application of some tests of element mobilization on the samples indicate that ocean-floor hydrothermal processes led to variable mobilization of large ion lithophile elements (LILE) such as

Ba, Rb, K, and Sr. By contrast, the transition metals (V, Cr, Mn, Fe, Co, Ni, and Zn), Mg, Y, and the high field strength (HFS) elements (Zr, Nb, Ti, Hf, P, and REE) remained relatively immobile and largely reflected magmatic abundances. For these reasons and following previous researchers (Pearce and Norry 1979; Shervais 1982; Beccaluva et al. 1983), we base this discussion on the geochemical and petrogenetic features of the studied rocks on elements that are immobile during metamorphic and alteration processes.

Central Mirdita Volcanics. Bortolotti et al. (1996) subdivided the central Mirdita volcanic rocks into four groups: (1) high-Ti basalts, (2) low-Ti basalt-basaltic andesite-dacite-rhyolite series, (3) medium-Ti basalts and basaltic andesites showing geochemical features intermediate between high- and low-Ti basalt, and (4) very low-Ti basaltic and basaltic andesite dikes. The major geochemical dif-

ferences among these groups lie in the different concentrations of high field strength elements (HFSE) such as P, Zr, Ti, and Y, as well as V, Cr, and Ni. The data presented in this article confirm these conclusions.

Group 1 basalts (high-Ti basalts) exhibit a wide range of variation in the Mg# value (68–44), where Mg# is defined as $100 \times \text{Mg}/(\text{Mg} + \text{Fe})$, although most of the samples are from moderately evolved magmas (Mg# = 60–50). They generally show uniform geochemical characteristics ($\text{TiO}_2 > 1.30$ wt %, Zr = 88–130 ppm, Y = 37–51 ppm, $\text{P}_2\text{O}_5 = 0.07\text{--}0.47$ wt %; table 1). Group 1 Ti/V ratios range from 25 to 44 (fig. 4) and cluster in the field for basalts generated at mid-ocean ridge settings (Beccaluva et al. 1983). Based on the relative distribution of HFSE concentrations (fig. 5A), these rocks show affinities with ocean-floor basalts. In particular, elements from Ta to Yb (fig. 5A) exhibit rather flat patterns ranging from one to five times N-MORB (Pearce 1983) contents. Group 1 basalts from the central Mirdita area show patterns for heavy REE (HREE) about 20–30 times chondritic abundances (fig. 5B) and a mild light REE (LREE) depletion ($\text{La}_N/\text{Sm}_N = 0.43\text{--}0.76$). The overall REE patterns presented by these basalts are consistent with N-MORB compositions. Magma evolution, probably occurring in a mid-ocean ridge open system, is indicated by the enrichment of FeO , TiO_2 , P_2O_5 , and V in the more evolved lavas (Beccaluva et al. 1995).

Group 2 volcanic rocks (low-Ti basalt-andesite-dacite-rhyolite series) largely characterize the eastern ophiolitic belt (Beccaluva et al. 1994; Bébien et al. 2000), though many occurrences are also found in the western belt. This series shows a clear IAT affinity, with TiO_2 contents ranging from 0.29 to 0.76 wt %, Zr = 5–106 ppm, Y = 11–27 ppm, and $\text{P}_2\text{O}_5 = 0.03\text{--}0.11$ wt % in the basaltic rocks. Mg# varies from 82 to 49 in basaltic rocks, extending to 35 in the more evolved lavas. The discrimination diagram of figure 4 confirms their IAT magmatic affinity. Actually, Shervais (1982) suggested that Ti/V ratios < 20 are consistent with genetic conditions typical of island arc settings. HFSE patterns (fig. 5C) are characterized by a general depletion, with respect to the N-MORB composition, approximately ranging from 0.2 to 0.8 times N-MORB. Figure 5C also demonstrates a slight relative depletion of Nb, P, and Ti with respect to the other incompatible elements in some basaltic samples. Basaltic rocks of the group 2 series from the central Mirdita area are characterized either by depletion or moderate enrichment in LREE with respect to medium REE (fig. 5D), as exemplified by the La_N/Sm_N ratios rang-

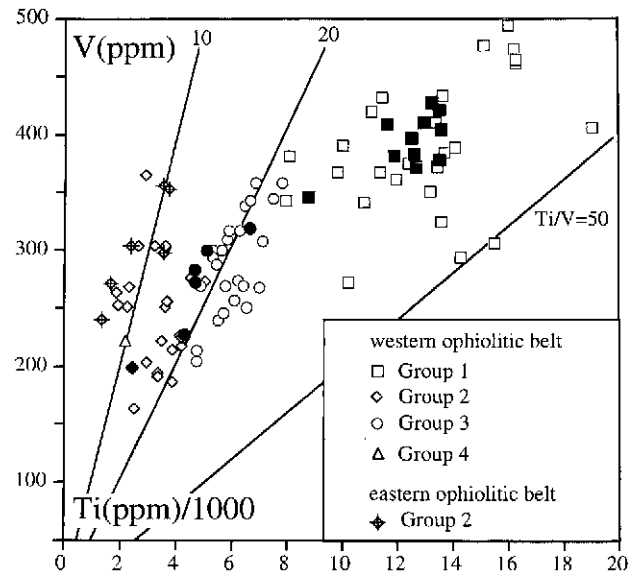


Figure 4. Ti/1000 versus V discrimination diagram (Shervais 1982) for mafic volcanic rocks from the central Mirdita area. Solid symbols indicate samples from the Kalur volcanic section.

ing from 0.15 to 1.76. HREE indicate small amounts of depletion (six to 15 times chondritic abundances) if compared to the group 1 basalts. Low-Ti rocks from the western and eastern belts are geochemically indistinguishable; nonetheless, in the Ti versus V diagram (fig. 4) it can be seen that eastern-belt basaltic rocks display Ti/V ratios generally lower than those in their western-belt equivalents.

Group 3 basalts (medium-Ti basalts) show geochemical characteristics that spread from those previously described in group 1 and group 2 basalts. In particular, the TiO_2 content varies from 0.70 to 1.32 wt %, Zr = 10–120 ppm, Y = 21–37 ppm, and $\text{P}_2\text{O}_5 = 0.01\text{--}0.16$ wt %. These transitional geochemical features are indicated in the Ti versus V discrimination diagram (fig. 4) as well as by the degree of depletion of HFSE with respect to N-MORB (fig. 5E). In particular, figure 5E shows a less pronounced HFSE depletion (0.5–1 times N-MORB) with respect to the group 2 basaltic rocks. Moreover, as is the case for group 2 basalts, a number of samples exhibit remarkable Th, U, Ta, Nb, La, and Ce depletion. The group 3 basaltic rocks are characterized by medium to heavy REE patterns (fig. 5F) similar to those of group 1 basalts (fig. 5B), although with smaller amounts of enrichment (10–15 times chondritic abundances). By contrast, group 3 is characterized by severe LREE depletion

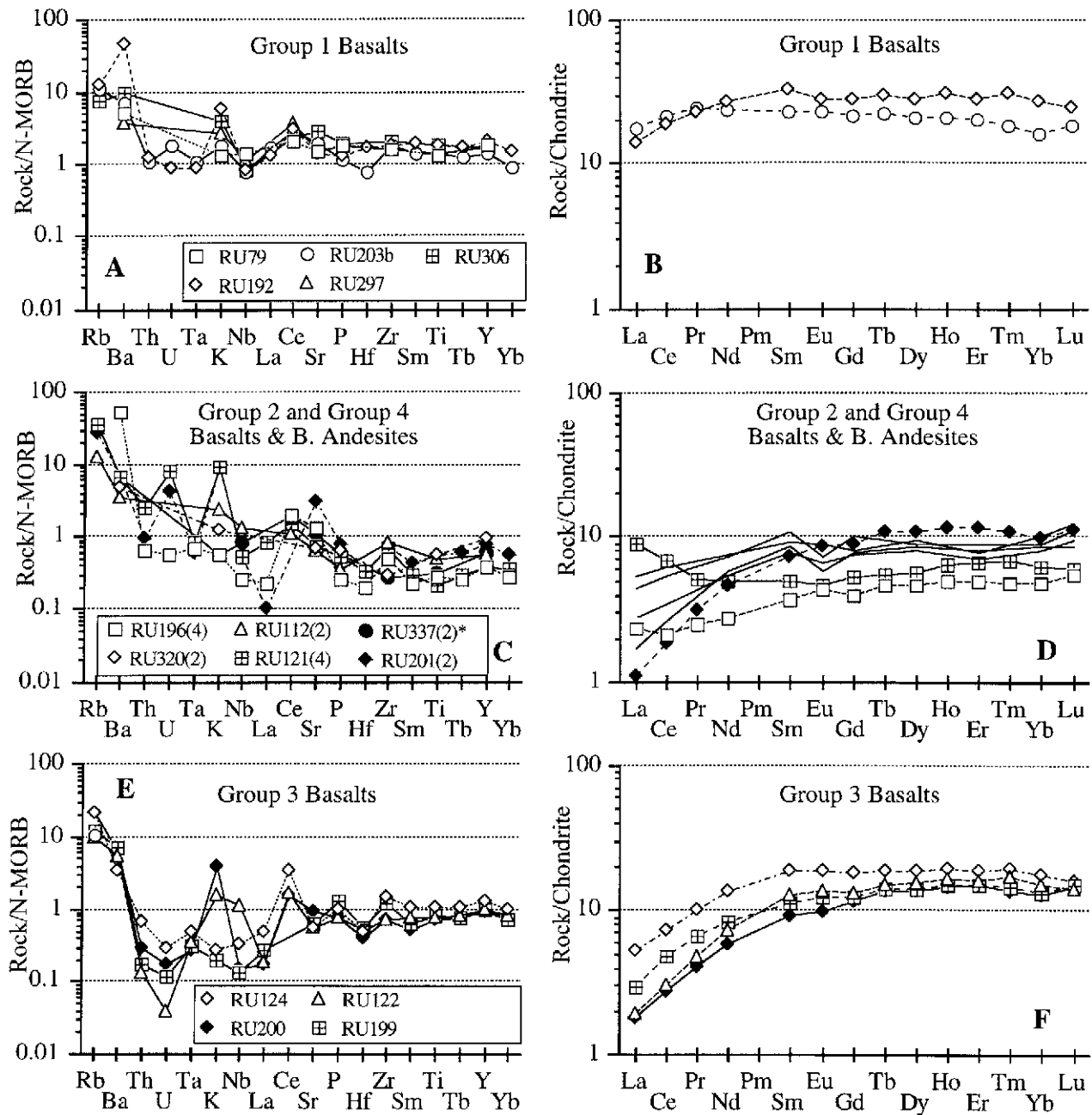


Figure 5. N-MORB normalized (Pearce 1983) incompatible trace element abundance diagrams and chondrite-normalized (Sun and McDonough 1989) REE patterns for selected samples from the western ophiolitic belt. The asterisk indicates a basalt from the eastern ophiolitic belt. In *D*, low-Ti basalts from the eastern ophiolitic belt (L. Beccaluva, unpublished data) are reported for comparison (*solid lines without symbols*).

($La_N/Sm_N = 0.15-0.28$). Despite the great variation of the geochemical characteristics of these basalts, the Mg# is surprisingly uniform (Mg# = 68–60), suggesting a scarce magmatic evolution. In summary, though the major elements do not permit a clear distinction between basalts generated in MOR or SSZ settings, the HFSE and REE unequivocally

indicate that the group 3 basalts bear SSZ magmatic features.

Group 4 basaltic rocks (very low-Ti basalts, basaltic andesites, and minor andesites) occur as dikes crosscutting all the previously described volcanic series. Basalts are typically characterized by very low TiO_2 (0.12–0.37 wt %) and Y (3–11 ppm) con-

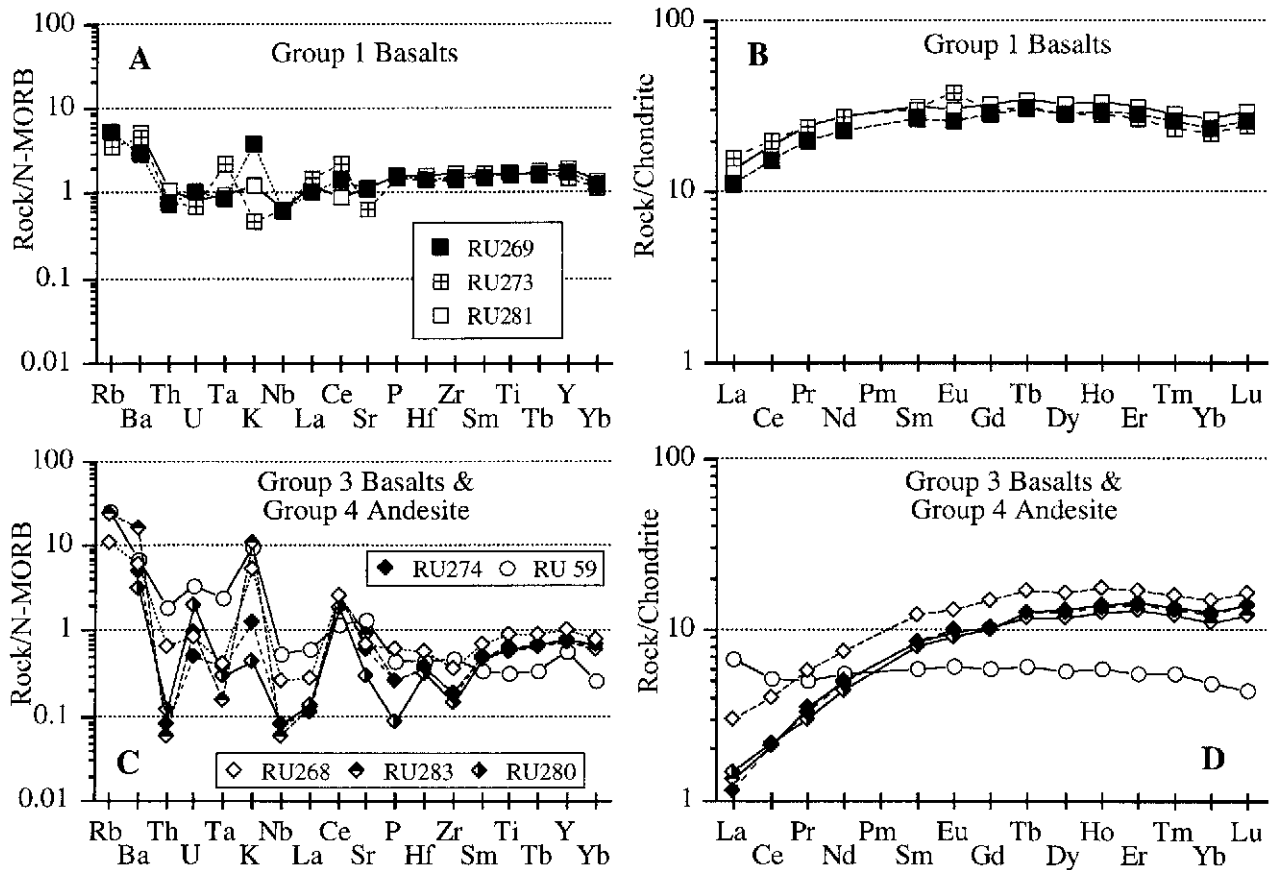


Figure 6. N-MORB normalized (Pearce 1983) incompatible trace element abundance diagrams and chondrite-normalized (Sun and McDonough 1989) REE patterns for selected samples from the Kalur volcanic section.

tents combined with high amounts of MgO (9.62–16.72 wt %) and CaO (9.87–11.91 wt %), with Mg# ranging from 79 to 53. Group 4 basalts are typically characterized by a boninitic-type REE pattern (fig. 5D) indicating a melt extraction from a severely depleted source or, alternatively, a very high degree of partial melting.

The Kalur Volcanic Section. We sampled and analyzed the Kalur volcanic section (fig. 3) in detail in order to investigate the geochemical variations along one of the best preserved parts of the western volcanic sequence and to explore the spatial and temporal relationships among high-Ti, low-Ti, and medium-Ti volcanic rocks. Whole rock compositions for Kalur volcanics are reported in table 2. We summarize the geochemical variations along this volcanic sequence in figure 3 by plotting the variation of some representative geochemical parameters along the stratigraphic sequence. From this figure, it is evident that group 1 basalts showing MORB affinity intercalate with group 3 basalts reflecting an SSZ influence. The most significant geo-

chemical features of group 1 basalts are TiO_2 contents >1.43 wt % and Ti/V ratios >25. Group 1 basalts from the Kalur section are similar to high-Ti basalts from other parts of the western belt (fig. 4). By contrast, group 3 basalts display TiO_2 contents <1.09 wt % and Ti/V ratios <20. Representative incompatible element abundances are presented in figures 6A and 6C. The HFSE contents in both group 1 and group 3 basalts are similar to those of the equivalent volcanics from the whole central Mirdita area (fig. 5A, 5E) and present the same general characteristics. The various types of Kalur volcanics can readily be distinguished by their REE patterns in figures 6B and 6D, which display the same characteristics already described for similar western-belt samples. Finally, the Kalur section is topped by a few meters of very low-Ti basaltic andesitic lava flow (group 4). The most distinguishing geochemical feature of this lava flow is the general REE depletion (five times chondritic abundances) and a moderate enrichment of LREE relative to me-

dium REE (fig. 6D) with La_N/Sm_N ratio = 1.12, which is similar to boninite-type REE patterns.

Pyroxene Chemistry

Clinopyroxene compositions are thought to be a suitable indicator of the magmatic affinity of basalts from different tectonic settings (Leterrier et al. 1982) and from different ophiolitic types (Beccaluva et al. 1989) since clinopyroxene chemistry, although controlled by crystal-chemical constraints, is strongly influenced by the composition of the magmas from which the basalts crystallize. Representative analyses of fresh clinopyroxene crystals are given in table 3.

In group 1 basalts, clinopyroxenes are restricted to interstitial or granular microlites in the groundmass. These phases lie mainly in the augite field, extending to diopsidic compositions (fig. 7A). The overall compositional range of group 1 basalt clinopyroxenes is similar to those documented in MOR basalts by Beccaluva et al. (1989). They exhibit marked Fe-enrichment trends (fig. 7A) and high TiO_2 contents (0.48–1.96 wt %), whereas Mg# varies from 84.9 to 60.5 (table 3). The Ti/Al ratio is assumed to vary as a function of the Ti-Al substitution in pyroxene, which, in turn, is strongly

controlled by the magma composition. Ti/Al ratios displayed by clinopyroxenes from group 1 basalts are always >0.16 .

The clinopyroxenes in the group 2 basalts, comprising phenocrysts, microphenocrysts, and groundmass microlites, are distinct from those in group 1 basalts since they lie predominantly in the magnesium-rich augite field, rarely extending to augitic compositions (fig. 7B). These phases are compositionally similar to those observed in SSZ ophiolites and in their modern analogues (Leterrier et al. 1982; Beccaluva et al. 1989). No Fe-enrichment trends are observed. TiO_2 contents (up to 1.43 wt %) are characteristically lower than those in group 1 basalt clinopyroxenes. By contrast, Mg# is significantly high (92.1–76.9), whereas Ti/Al ratios in clinopyroxenes from group 2 basalts are <0.09 .

Clinopyroxenes from group 3 basalts are found as microphenocrysts and groundmass microlites. Compositionally, they mainly lie across the magnesium-rich augite–augite boundary (fig. 7C). Their chemical characteristics are intermediate between the first two groups. In fact, moderate Fe-enrichment trends are observed in some samples, TiO_2 ranges from 0.20 to 1.02 wt %, Mg# is included between 89.7 and 56.5, and Ti/Al ratios range from 0.05 to 0.19.

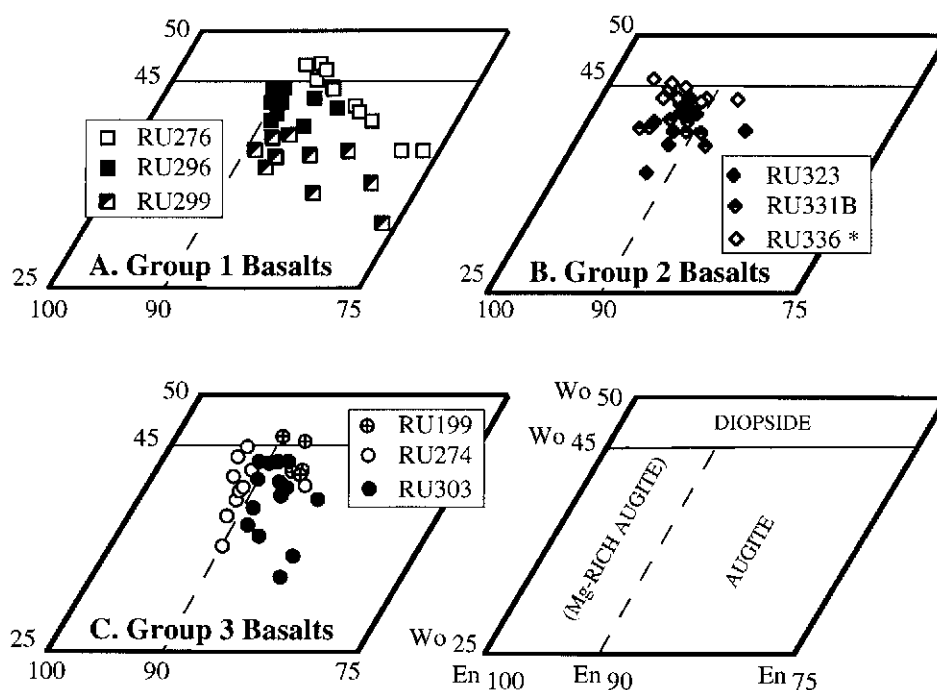


Figure 7. Groundmass and phenocryst clinopyroxene compositions, expressed in term of wollastonite-enstatite-ferrosilite, in basaltic rocks from the central Mirdita area. Asterisk indicates a sample from the eastern ophiolitic belt. Pyroxene nomenclature is from Morimoto (1989).

The compositional correspondence of the clinopyroxenes analyzed in this study with those from modern oceanic analogues is shown in the discrimination diagram of figure 8 (Beccaluva et al. 1989), where clinopyroxenes from group 1 and group 2 basalts plot in the MORB and IAT fields, respectively. Clinopyroxenes from group 3 basalts, although plotting in the IAT field, once again display compositions shifted toward the MORB field when compared with those of the group 2 basalts.

Petrogenesis

One of the main objectives of this study has been to evaluate the role of SSZ (i.e., arc) processes in forming the western-belt crust. It is commonly accepted that the SSZ signature may have two basic features: the depleted signature, as a consequence of previous melt extraction in the mantle source (i.e., MORB generation), and the LILE-enrichment signature, which is produced by subduction-derived fluids. The latter is, however, difficult to identify in ophiolitic rocks since they are commonly altered. In particular, variable amounts of LILE mobilization have been observed in the studied rocks, in keeping with the relative variation of these elements with respect to Mg# and Zr variation.

The differences between the lava types analyzed in this article could be related to different source characteristics, since the variation in lava chemistry is a function of mantle composition rather than shallow-level crustal processes (Pearce and Norry 1979; Pearce et al. 1984). According to the models proposed by Pearce and Norry (1979) and Kostopoulos and Murton (1992), the particular disparity in petrochemical character observed among some western-belt volcanic sequences (e.g., the Kalur sequence) strongly indicates the contemporaneous presence of independent magma sources and, most likely, does not reflect either the extent of partial melting or fractionation of a single magma source.

The depletion of HFSE (e.g., Ta, Nb, Ti) and REE relative to N-MORB has long been recognized as a distinguishing characteristic of subduction-related magmas. Such a geochemical signature is commonly interpreted as a consequence of multistage mantle depletion. HFSE and REE patterns of selected samples from the western belt and, in particular, from the Kalur volcanic section (fig. 5A, 5B; fig. 6A, 6B) indicate that the group 1 basalts are consistent with MORB compositions. By contrast, observing the incompatible elements and REE abundance in figures 5 and 6, we notice a progressive depletion of LILE, HFSE, and LREE from group

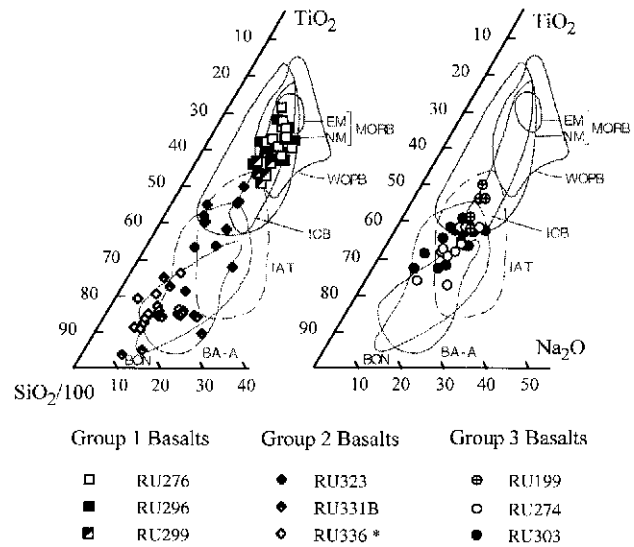


Figure 8. $\text{TiO}_2\text{-Na}_2\text{O-SiO}_2/100$ (wt %) discrimination diagram (Beccaluva et al. 1989) for clinopyroxene from central Mirdita area basaltic rocks. Fields representing clinopyroxene compositions in basalts from modern oceanic settings are reported for comparison. NM = normal MORB; EM = enriched MORB; ICB = Iceland basalts; IAT = island arc tholeiites; BON = boninites; BA-A = intraoceanic fore-arc basalts and basaltic andesites. Asterisk indicates a sample from the eastern ophiolitic belt.

1 (high-Ti) to group 3 (medium-Ti) basalts. This depletion is followed by a successive depletion of HFSE and REE coupled with a relative enrichment in LILE, toward group 2 (low-Ti) and group 4 (boninitic) basaltic rocks. In addition, group 4 varieties exhibit less pronounced LREE depletion or LREE enrichment relative to medium REE.

The strongly depleted LILE and LREE and poorly depleted HREE patterns (figs. 5F, 6D) displayed by group 3 basalts ($\text{La}_N/\text{Sm}_N = 0.15\text{--}0.28$, $\text{HREE} = 10\text{--}15 \times \text{chondrite}$) suggest that these basalts originated from partial melting of refractory mantle sources. Similar REE patterns can be observed in many SSZ basalts (Klein and Karsten 1995; Karsten et al. 1996; Yumul 1996) and are interpreted as the product of partial melting of a SSZ mantle wedge that underwent a previous melt extraction in an MOR setting. In addition, the marked LREE depletion (figs. 5F, 6D) displayed by the group 3 basalts, coupled with the considerable Ta and Nb depletion (figs. 5E, 6C), suggests that the SSZ mantle wedge did not undergo any significant enrichment due to subduction-related fluids. By contrast, group 2 and group 4 rocks, although generally depleted in incompatible elements, show less pronounced Th, U,

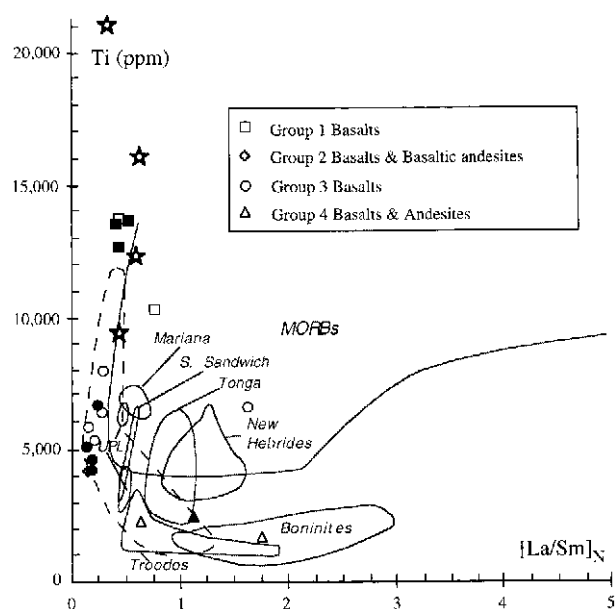


Figure 9. $(La/Sm)_N$ versus Ti diagram for basalts, basaltic andesites, and andesites from the western ophiolitic belt (simplified after Beccaluva and Serri 1988). MORBs and boninites from various localities, boninites from Troodos, as well as IAT data for New Hebrides, Tonga, South Sandwich, Mariana Fore-arc, and Troodos upper pillow lavas (UPL) (see Beccaluva and Serri 1988 for references) are reported for comparison together with data from Beccaluva et al. (1994) for western-belt high-Ti basalts (stars) and eastern-belt low-Ti basalts (dashed field).

Ta, and Nb, as well as more conspicuous HREE depletion, when compared with group 3 basalts (fig. 5). This may be interpreted as resulting from greater degrees of partial melting of more refractory mantle sources possibly enriched by subduction-derived fluids, as evidenced by the La_N/Sm_N ratios (0.64–1.76) in boninitic rocks.

Figure 9, in which the $(La/Sm)_N$ ratios are plotted against Ti, shows that group 2 and group 3 basalts have lower $(La/Sm)_N$ ratios than group 1 basalts. According to Beccaluva and Serri (1988), such ratios are compatible with high degrees of hydrous (but not necessarily water-saturated) melting of mantle sources that experienced previous extraction of basaltic melts without significant subduction-derived enrichment events. The group 4 rocks, although characterized by rather uniform Ti content, display variable $(La/Sm)_N$ ratios comparable to those of typical boninites (fig. 9) and reflect various degrees of enrichment.

The degree of depletion of the mantle source(s) can be inferred by plotting a compatible versus an

incompatible element. The compatible element abundance is not significantly modified during the progressive mantle source depletion. By contrast, the abundance of incompatible elements is closely related to the source depletion.

Our purpose is to relate the mafic magma compositions from the central Mirdita ophiolites, with particular regard to the western ophiolitic belt, to the degree of depletion of their possible mantle parents. For this reason, we applied the fractional melting (or incremental melting with small increments) modeling adopted by Pearce et al. (1992) for the Bonin-Mariana fore-arc. In this modeling, we choose Mg# as representing compatible element behavior and TiO_2 as the incompatible element, since TiO_2 is not likely to have been added to the source by subduction-derived components. According to Pearce et al. (1992), in the Mg# versus TiO_2 diagram of figure 10, the theoretical mantle residue compositions from a fertile MORB mantle identify an almost horizontal trend. Figure 10 also reports the fractional melting trend defined by accumulated fractional melts from a fertile MORB mantle, calculated for 10% fractional melting of mantle previously depleted by loss of 0%, 5%, 10%, 15%, and 20% of melt. This diagram is somewhat affected by the source composition postulated in the model,

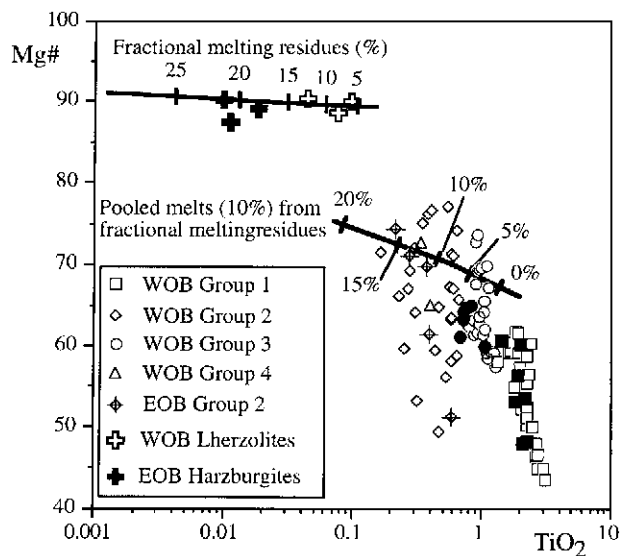


Figure 10. TiO_2 versus Mg# diagram for the central Mirdita basalts and basaltic andesites (after Pearce et al. 1992). Solid symbols indicate samples from the Kalur volcanic section. Data for selected unaltered western-belt lherzolites and eastern-belt harzburgites are from Beccaluva et al. (1994). WOB = western ophiolitic belt; EOB = eastern ophiolitic belt.

nonetheless, it can provide a good estimation of the average degree of depletion of the various sources for the western-belt lava types. In particular, the compositions of group 1 basalts fit best with 10% melting of an undepleted fertile MORB mantle. The group 3 suite may be derived from 10% melting of a mantle that previously experienced about 5% of previous melting. Finally, the group 2 suite, having the lowest TiO₂ content, may be derived from 10% partial melting of a mantle source previously depleted by approximately 7%–17% melting. The western-belt mantle lherzolites are thought to be the mantle parents of the group 1 and, possibly, of the group 3 basalts, whereas the eastern-belt mantle harzburgites likely represent the residues from the generation of group 2 and group 4 magmatic suites. The plot of selected fresh mantle peridotites from both western and eastern ophiolitic belts in figure 10 confirms this assumption. In particular, western-belt lherzolites represent the residues from 7%–12% partial melting, while eastern-belt harzburgites are the residues after 17%–22% melt extraction.

Discussion

Beccaluva et al. (1994) and Bortolotti et al. (1996) pointed out that the eastern-belt volcanic series is almost exclusively characterized by low-Ti and boninitic volcanic sequences, reflecting a supra-subduction origin for these ophiolites. By contrast, in accordance with Bortolotti et al. (1996), the data presented in this article indicate that volcanic rocks from the western belt, though largely characterized by MORB sequences, also contain group 2 and/or group 3 basalts spatially juxtaposed to or interlayered with MORBs at several localities in the central Mirdita area. The best example of such relationships is represented by the Kalur volcanic sequence, where high-Ti basalts alternate with basalts showing transitional characteristics (fig. 3), while the top of the volcanic sequence is represented by an andesitic massive lava flow displaying a boninitic geochemical affinity. A general trend of evolution from high-Ti basalts toward subduction-related magmas is identified in the Kalur section. Similar rough evolutionary trends are also recognized in other adjacent volcanic sequences, where boninitic dikes are also locally found.

Spatial or temporal modification of the magmatic affinity in ophiolites has been described by some authors (Geary et al. 1989; Klein and Karsten 1995; Karsten et al. 1996; Yumul 1996). In all cases, the magmatic changes follow specific trends according to the variation of the geodynamic settings of the

primary magma source through space or time. Typical examples are represented by the evolution from IAT to MORB compositions during the incipient opening of back-arc basins. Alternatively, the passage from MORB to IAT is commonly related to processes that produce chemical modification of older oceanic crust in a fore-arc setting during the early stages of island arc formation. However, all these models imply a considerable difference in age between the different ophiolitic types such as, for example, in the Coast Range ophiolites (Shervais and Kimborough 1985), where a Middle Jurassic island arc association is related to Late Jurassic ophiolites with oceanic affinity.

In contrast, ⁴⁰Ar/³⁹Ar geochronology (Vergély et al. 1998) and radiolarian age (Marcucci and Prela 1996) of the Albanian ophiolites and related metamorphic soles indicates that MORB and SSZ crustal accretions were approximately contemporaneous. Moreover, the mineralogical and whole rock geochemical data presented in this article support the hypothesis that part of the western ophiolitic belt formed in an environment in which both MORB and IAT magmas coexisted both spatially and temporally.

In this context, Bébien et al. (2000) concluded that the different magmatic suites in the Albanian ophiolites cannot be related to different stages of evolution and tectonic settings (either MOR or SSZ settings). In their model, Bébien et al. (2000) suggest that Albanian ophiolites were generated on the whole during an early stage of subduction. However, this conclusion contrasts with the general consensus that in the Albanian ophiolites (Beccaluva et al. 1994; Shallo 1994; Cortesogno et al. 1998) and, in general, all the Dinaride-Hellenide ophiolites (Jones et al. 1991; Robertson and Shallo 2000), the high-Ti and low-Ti ophiolitic belts reflect two distinct original geodynamic settings, MOR and SSZ, respectively.

Beccaluva et al. (1995, 1998) demonstrated that the western-belt ophiolites originated by fractional crystallization, in prevalently open systems, from MORB parental magmas generated in an MOR setting under anhydrous conditions. They came to this conclusion by observing that the more primitive magmas from the western belt are geochemically similar to the experimental liquids obtained by Hirose and Kushiro (1993) from the melting of a spinel lherzolite under anhydrous conditions. Moreover, the fractionation trend observed for the western-belt volcanics is compatible with the model proposed by Hirose and Kushiro (1993). Beccaluva et al. (1995, 1998) also concluded that the eastern-belt ophiolites evolved through frac-

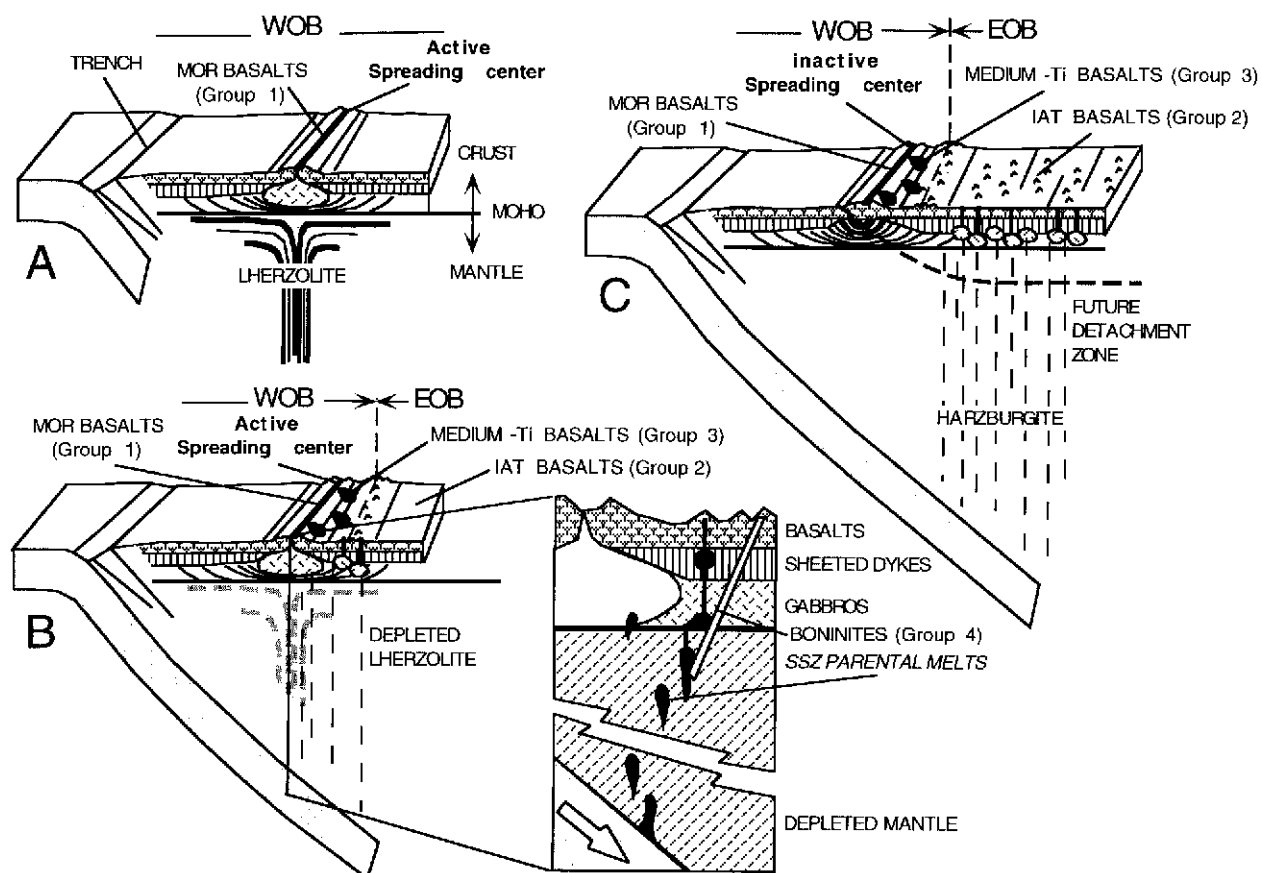


Figure 11. Schematic geodynamic model for interaction of mid-ocean ridge and subduction-related processes at the infant intraoceanic arc setting for Albanian ophiolites. See text for explanations. *WOB* = western ophiolitic belt; *EOB* = eastern ophiolitic belt.

tional crystallization, in closed systems, from low-Ti picritic parental magmas generated in a SSZ mantle wedge characterized by moderately hydrous conditions. This conclusion was reached by observing the close geochemical similarity between the primitive magmas from the eastern belt and the primitive experimental liquids obtained by Hirose and Kawamoto (1995) from the melting of a mantle peridotite under moderately hydrous conditions ($H_2O = 0.1$ wt %). Moreover, the fractionation trend of the eastern-belt volcanics is compatible with the model proposed by Hirose and Kawamoto (1995) and is similar to that described by Thy and Xenophontos (1991) for the Troodos lava series.

Nonetheless, we need a more complex tectonomagmatic scenario to explain the general trend of geochemical transition from group 1 (high-Ti) to group 2 (low-Ti) volcanics via group 3 (medium-Ti) basalts recognized in some of the western-belt volcanic sequences and to explain the chemical differences between western-belt lava types. Taking

into account the results of Beccaluva et al. (1995, 1998) and the data presented in this article, we suggest the following tectonomagmatic evolution for Albanian ophiolites.

Initially, the western-belt crust formed at a normal oceanic spreading center (fig. 11A). Soon after, subduction initiated nearby, trapping hot oceanic lithosphere in a proto-fore-arc (infant arc) setting (fig. 11B). Two-dimensional experimental modeling (Insergueix-Filippi et al. 2000) indicates that the initiation of subduction near an active ridge axis does not immediately stop the ascending asthenospheric flow but leads to a deviation of its upper part in the same direction as the subducting lithosphere. According to this model, the subduction of hot, young lithosphere and the incipient dehydration of the altered oceanic crust leads to thermal perturbation of the overlying upper mantle wedge, producing partial melting of localized mantle portions that have previously experienced MORB melt extraction. This partial melting generates primitive

magmas with SSZ signatures (i.e., HFSE and REE depleted features) such as the group 3 basalts. In more rare instances, we observe LILE and LREE relative enrichments that are likely related to fluids driven off the subduction zone. These magmas were then extruded contemporaneously with the last group 1 basalts related to the progressive extinction of MORB magmatism (fig. 11B).

The geochemical variations observed among the western-belt volcanic sequences are consistent with partial melting of increasingly refractory mantle sources further locally enriched by subduction-derived fluids. Consequently, the early group 2 and group 4 volcanics were produced from partial melting of strongly depleted sources. At this stage (fig. 11B), group 2 and group 4 volcanics were contemporaneous with the declining group 3 basalts and heralded the initiation of island arc magmatism, which resulted in the development of the eastern-belt ophiolitic sequences (fig. 11C).

It is commonly accepted that boninite melts originate from strongly depleted harzburgites mixed with an enriched component. The sources of the enriched component are, in most cases, subducted sediments and basalts (Hikey and Frey 1982; Cameron et al. 1983; Bloomer 1987; Stern et al. 1991). Melting of highly refractory peridotites results from the combined effects of subduction-related fluids and an unusually high thermal regime, such as that occurring beneath young oceanic crusts. Consequently, boninite magmas almost exclusively form in subduction settings that are not in thermal equilibrium, as, for instance, during the initiation of subduction (Stern et al. 1991). According to this conclusion, the boninitic magmatism produced in the Albanian ophiolites may be related to the high thermal regime of the young suprasubduction lithosphere in proximity to an extinguishing mid-ocean ridge.

On account of constraints imposed by subduction geometries and thermal regime, the formation of boninitic magma types occurred in the proto-fore-arc crust closest to the trench shortly after the initiation of subduction, according to the model proposed by Hikey and Frey (1982) and Stern et al. (1991). An alternative model for explaining the coexistence of the magmatic associations observed in the western belt may consider the development of a back-arc, since MOR and SSZ magma pairings may be observed in arc-back-arc settings. Nonetheless, some evidence argues against the hypothetical formation of the Albanian ophiolites in this setting.

1. The development of a back-arc setting is gen-

erally marked by a transition from SSZ to MORB-like magmatism, while in the Albanian ophiolites, a transition from MORB to SSZ magmatism is recorded.

2. The Jurassic top-to-west tectonic transport direction observed in the common metamorphic sole of both ophiolitic belts suggests the eastward direction of the subduction. An eastward subduction implies that, if the MORB-like associations of the western belt are referred to a back-arc setting, they should be located in an easternmost position with respect to the SSZ ophiolitic series, in contrast to what is observed.

3. The presence of the same subophiolitic mélange (Rubik Complex) at the base of the metamorphic sole also suggests an eastward direction of the subduction and further supports the hypothesis that part of the MOR ophiolites should have been located to the East with respect to the trench, thus above the subduction plane (fig. 11).

4. The MOR and SSZ sequences from Albania are almost coeval. In a model implying an arc-back-arc setting, the MOR sequence should be younger than the boninitic magmatism.

5. Boninites are very rare in back-arc settings, while they are commonly found in fore-arc regions (Stern et al. 1991).

Conclusion

Albanian ophiolites, in particular the western ophiolitic belt, represent an original example of the complexity of magmatic processes developed during the infancy of arc settings. The interaction between an MOR magmatism in extinction and the initiation of SSZ magmatism can produce ophiolitic sequences where different magmatic associations showing distinctive geochemical features coexist either spatially or temporally. The model presented in this article can be useful for interpreting other ophiolitic sequences with complex geochemical features, with particular regard to the eastern Mediterranean ophiolites.

ACKNOWLEDGMENTS

This research was supported by Ministers Istruzione, Università e Ricerca and by Consiglio Nazionale delle Ricerche, Istituto di Geoscienze e Georisorse, Pisa. We thank L. Beccaluva for his comments on the manuscript and R. Tassinari and F. Olmi for chemical analyses. The authors are also obliged to P. Thy and an anonymous referee for their critical reviews.

REFERENCES CITED

- Aubouin, J.; Blanchet, R.; Cadet, P.; Celet, P.; Charvet, J.; Chorovic, J.; Cousin, M.; and Rampnoux, J. P. 1970. Essai sur la géologie des Dinarides. *Bull. Soc. Géol. Fr.* 12:1060–1095.
- Bébien, J.; Dimo-Lahitte, A.; Vergély, P.; Insergueix-Filippi, D.; and Dupeyrat, L. 2000. Albanian ophiolites. I. Magmatic and metamorphic processes associated with the initiation of a subduction. *Ofoliti* 25: 39–45.
- Bébien, J.; Shallo, M.; Manika, K.; and Gega, D. 1998. The Shebenik Massif (Albania): a link between MOR- and SSZ-type ophiolites? *Ofoliti* 23:7–15.
- Beccaluva, L.; Coltorti, M.; Ferrini, V.; Saccani, E.; Siena, F.; and Zeda, O. 1998. Petrological modelling of Albanian ophiolites with particular regard to the Bulqiza chromite ore deposits. *Period. Mineral.* 67:7–23.
- Beccaluva, L.; Coltorti, M.; Premti, I.; Saccani, E.; Siena, F.; and Zeda, O. 1994. Mid-ocean ridge and supra-subduction affinities in ophiolitic belts from Albania. *In* Beccaluva, L., ed. Special issue on Albanian ophiolites: state of the art and perspectives. *Ofoliti* 19: 77–96.
- . 1995. High-Ti and low-Ti ophiolitic belts in Albania: a petrogenetic model for crustal accretion in mid-ocean ridge and supra-subduction oceanic settings. *In* International Ophiolite Symposium, Pavia (Italy), Sept. 18–23, 1995. Symposium Proceedings 13–14.
- Beccaluva, L.; Di Girolamo, P.; Macciotta, G.; and Morra, V. 1983. Magma affinities and fractionation trends in ophiolites. *Ofoliti* 8:307–324.
- Beccaluva, L.; Macciotta, G.; Piccardo, G. B.; and Zeda, O. 1989. Clinopyroxene compositions of ophiolite basalts as petrogenetic indicator. *Chem. Geol.* 77:165–182.
- Beccaluva, L., and Serri, G. 1988. Boninitic and low-Ti subduction-related lavas from intraoceanic arc-back-arc systems and low-Ti ophiolites: a reappraisal of their petrogenesis and original tectonic setting. *Tectonophysics* 146:291–315.
- Bloomer, S. H. 1987. Geochemical characteristics of boninite- and tholeiite-series volcanic rocks from the Mariana forearc and the role of an incompatible element-enriched fluid in arc petrogenesis. *Geol. Soc. Am. Spec. Pap.* 215:151–164.
- Bortolotti, V.; Kodra, A.; Marroni, M.; Mustafa, F.; Pandolfi, L.; Principi, G.; and Saccani, E. 1996. Geology and petrology of ophiolitic sequences in the Mirdita region (northern Albania). *Ofoliti* 21:3–20.
- Cameron, W. E.; McCulloch, M. T.; and Walker, D. A. 1983. Boninite petrogenesis: chemical and Nd-Sr isotopic constraints. *Earth Planet. Sci. Lett.* 65:75–89.
- Carosi, R.; Cortesogno, L.; Gaggero, L.; and Marroni, M. 1996. Geological and petrological features of the metamorphic sole from the Mirdita ophiolites, northern Albania. *Ofoliti* 21:21–40.
- Cortesogno, L.; Gaggero, L.; Jaho, E.; Marroni, M.; Pandolfi, L.; and Shtjefanaku, D. 1998. The gabbroic complex of the western ophiolitic belt, northern Albania: an example of multilayered sequence in an intermediate-spreading oceanic ridge. *Ofoliti* 23: 49–64.
- Geary, E. E.; Kay, R. M.; Reynolds, J. C.; and Kay, S. M. 1989. Geochemistry of mafic rocks from the Coto Block, Zambesi ophiolite, Philippines: trace element evidence for two stages of crustal growth. *Tectonophysics* 168:43–63.
- Hikey, R., and Frey, F. A. 1982. Geochemical characteristics of boninite series volcanics: implications for their sources. *Geochim. Cosmochim. Acta* 46:2099–2115.
- Hirose, K., and Kawamoto, T. 1995. Hydrous partial melting lherzolite at 1 Gpa: the effect of H₂O on the genesis of basaltic magmas. *Earth Planet. Sci. Lett.* 133:463–473.
- Hirose, K., and Kushiro, I. 1993. Partial melting of dry peridotites at high pressures: determination of compositions of melts segregated from peridotite using aggregates of diamonds. *Earth Planet. Sci. Lett.* 114: 477–489.
- Insergueix-Filippi, D.; Dupeyrat, L.; Dimo-Lahitte, A.; Vergely, P.; and Bébien, J. 2000. Albanian ophiolites. II. Model of subduction zone infancy at a mid-ocean ridge. *Ofoliti* 25:47–53.
- Jones, G.; Robertson, A. H. F.; and Cann, J. R. 1991. Genesis and emplacement of the supra-subduction zone Pindos ophiolite, northwestern Greece. *In* Peters, T. J.; Nicolas, A.; and Coleman, R. G., eds. Ophiolite genesis and evolution of the oceanic lithosphere: proceedings of the Ophiolite Conference, Muscat, Oman, January 7–18, 1990. Dordrecht, Kluwer Academic, p. 771–799.
- Karsten, J. L.; Klein, E. M.; and Sherman, S. B. 1996. Subduction zone geochemical characteristics in ocean ridge basalt from the southern Chile Ridge: implications of modern ridge subduction systems for the Archean. *Lithos* 37:143–161.
- Klein, E. M., and Karsten, J. L. 1995. Ocean-ridge basalts with convergent-margin geochemical affinities from the Chile Ridge. *Nature* 374:52–57.
- Kostopoulos, D. K., and Murton, B. J. 1992. Origin and distribution of components in boninite genesis: significance of the OIB component. *In* Parson, L. M.; Murton, B. J.; and Browning, P., eds. Ophiolites and their modern oceanic analogues. *J. Geol. Soc. Lond. Spec. Pap.* 60:133–154.
- Leterrier, J.; Maury, R. C.; Thonon, P.; Girard, D.; and Marchal, M. 1982. Clinopyroxene composition as a method of identification of the magmatic affinities of paleo-volcanic series. *Earth Planet. Sci. Lett.* 59:139–154.
- Marcucci, M., and Prella, M. 1996. The Lumi i zi, (Puke) section of the Kalur Cherts: radiolarian assemblages and comparison with other sections in northern Albania. *Ofoliti* 21:71–76.

- Morimoto, N. 1989. Nomenclature of pyroxenes. *Can. Mineral.* 27:143–156.
- Pearce, J. A. 1983. Role of the sub-continental lithosphere in magma genesis at active continental margin. *In* Hawkesworth, C. J., and Norry, M. J., eds. *Continental basalts and mantle xenoliths*. Nantwich, Shiva, p. 230–249.
- Pearce, J. A.; Lippard, S. J.; and Roberts, S. 1984. Characteristics and tectonic significance of supra-subduction ophiolites. *In* Kokelaar, B. P., and Howells, M. F., eds. *Marginal basin geology*. *Geol. Soc. Lond. Spec. Publ.* 16:777–794.
- Pearce, J. A., and Norry, M. J. 1979. Petrogenetic implications of Ti, Zr, Y, and Nb variations in volcanic rocks. *Contrib. Mineral. Petrol.* 69:33–47.
- Pearce, J. A.; van der Laan, S. R.; Arculus, R. J.; Murton, B. J.; Ishii, T.; Peate, D. W.; and Parkinson, I. J. 1992. Boninite and harzburgite from Leg 125 (Bonin-Mariana forearc): a case study of magma genesis during the initial stage of subduction. *Proc. ODP, Sci. Results* (Fryer, P.; Coleman, P.; Pearce, J. A.; and Stokking, L. B., eds.) 125, College Station, Tex. (Ocean Drilling Program), p. 623–659.
- Rassios, A.; Beccaluva, L.; Bortolotti, V.; Mavrides, A.; and Moores, E. M. 1983. The Vourinos ophiolitic complex. *Ofioliti* 8:275–292.
- Robertson, A. H. F., and Dixon, J. E. 1984. Introduction: aspects of the geological evolution of the eastern Mediterranean. *In* Dixon, J. E., and Robertson, A. H. F., eds. *The geological evolution of the eastern Mediterranean*. *Geol. Soc. Lond. Spec. Publ.* 49:1–73.
- Robertson, A. H. F., and Shallo, M. 2000. Mesozoic-Tertiary evolution of Albania in its regional eastern Mediterranean context. *Tectonophysics* 316:197–254.
- Rochette, P.; Jenatton, L.; Dupuy, C.; Boudier, P.; and Reuber, I. 1991. Diabase dikes emplacement in the Oman ophiolite: a magnetic fabric study with reference to geochemistry. *In* Peters, T. J.; Nicolas, A.; and Coleman, R. G., eds. *Ophiolite genesis and evolution of the oceanic lithosphere: proceedings of the Ophiolite Conference, Muscat, Oman, January 7–18, 1990*. Dordrecht, Kluwer Academic, 55–82.
- Shallo, M. 1994. Outline of the Albanian ophiolites. *In* Beccaluva, L., ed. *Special issue on Albanian ophiolites: state of the art and perspectives*. *Ofioliti* 19:57–75.
- Shervais, J. W. 1982. Ti-V plots and the petrogenesis of modern and ophiolitic lavas. *Earth Planet. Sci. Lett.* 59:101–118.
- Shervais, J. W., and Kimbrough, D. L. 1985. Geochemical evidence from the tectonic setting of the Coast Range ophiolite: a composite island arc-oceanic crust terrane in western California. *Geology* 13:35–38.
- Stern, R. J.; Morris, J.; Bloomer, S. H.; and Hawkins, J. W., Jr. 1991. The source of the subduction component in convergent margin magmas: trace element and radiogenic isotope evidence from Eocene boninites, Mariana forearc. *Geochim. Cosmochim. Acta* 55:1467–1481.
- Sun, S.-S., and McDonough, W. F. 1989. Chemical and isotopic systematics of ocean basalts: implications for mantle composition and processes. *In* Saunders, A. D., and Norry, M. J., eds. *Magmatism in the ocean basins*. *J. Geol. Soc. Lond. Spec. Pap.* 42:313–346.
- Thy, P., and Xenophontos, C. 1991. Crystallization order and phase chemistry of glassy lavas from the pillow sequence, Troodos ophiolites, Cyprus. *J. Petrol.* 32:403–428.
- Vergély, P.; Dimo, P.; and Monié, P. 1998. Datation des semelles métamorphiques ophiolitiques d'Albanie par la méthode $^{40}\text{Ar}/^{39}\text{Ar}$: conséquences sur le mécanisme de leur mise en place. *C. R. Acad. Sci. Paris* 326:717–722.
- Yumul, G. P. 1996. Varying mantle source of supra-subduction zone ophiolites: REE evidence from the Zambesi Ophiolite Complex, Luzon, Philippines. *Tectonophysics* 262:243–262.